# The XENON100 Detector for Dark Matter Searches

*Alexander Kish* for the XENON100 collaboration
University of Zürich, Winterthurerstrasse 190, 8057 Zürich, Switzerland

**DOI:** http://dx.doi.org/10.3204/DESY-PROC-2009-05/kish_alexander

The XENON100 detector, which has replaced the XENON10 prototype in the same location and improved shield at Laboratori Nazionali del Gran Sasso (Italy), is a dual phase (liquid-gas) xenon time-projection chamber for particle detection. The total amount of liquid xenon is 165 kg, of which 65 kg are in the target volume enclosed by a teflon/copper structure, the rest being in the surrounding active veto. The direct and proportional VUV light signal produced by particle interactions is detected by 242 PMTs. The expected sensitivity of the XENON100 for spin-independent WIMP-nucleon couplings is $2{\cdot}10^{-45}$ cm$^2$ for a 100 GeV WIMP with a background-free exposure of 6000 kg·days. In this paper, the principle of the XENON experiment and its main components are described, and a Monte Carlo study of the various types and sources of the background is summarized.

## 1 Introduction

The XENON100 detector [1], which is installed in the Laboratori Nazionali del Gran Sasso (LNGS) in Italy, is a second generation detector within the XENON program which aims at the direct detection of particle dark matter in the form of Weakly Interacting Massive Particles (WIMPs) [2], [3]. It is the successor of XENON10, which has set a limit on the WIMP-nucleon spin-independent cross-section of $8.8{\times}10^{-44}$ cm$^2$ for a WIMP mass of 100 GeV/c$^2$ [4]. XENON100 aims to improve this sensitivity by more than one order of magnitude due to increase of the target mass by a factor of 10 and reduction of the background in the target volume by a factor of 100.

The noble gas xenon has many advantages for particle detection, and in particular for dark matter search. It is an efficient and fast scintillator: $\lambda = 178$ nm, decay time of the fast (slow) component is 2.2 ns (27 ns) [5]. Availability of both scintillation and ionization signals provides event-by-event discrimination based on the amount of signals in both channels. High density of liquid xenon ($\sim 3$ g/cm$^3$) provides powerful self-shielding in a compact detector geometry, in addition to the absence of the naturally occurring long-lived radioactive isotopes.

## 2 XENON100 Detector and Shield Design

The XENON100 shield (schematically shown in figure 1, with $4\pi$ coverage of the detector, consists (from outside to inside) of tanks filled with water (thickness 20 cm) to moderate ambient neutrons, two layers of lead (15 cm outer layer and 5 cm inner layer with a lower contamination of the radioactive isotope $^{210}$Pb), 20 cm of polyethylene, and a 5 cm thick copper layer.

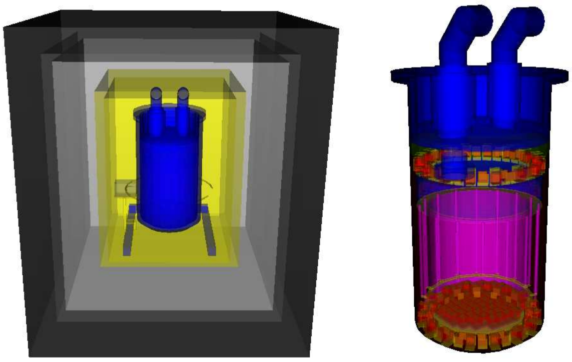

Figure 1: Left: The XENON100 detector inside its shield as it was simulated within the GEANT4 framework (the colors represent: two layers of lead - dark grey, polyethylene - light grey, and copper - yellow, water tanks are not shown; on the left side of the cryostat - lead brick for calibration with Am-Be source); Right: The closeup view of the detector (blue - stainless steel, magenta - PTFE, yellow - copper, orange - PMTs).

The XENON100 detector is a dual phase (liquid-gas) time-projection chamber (TPC). The total amount of liquid xenon (LXe) enclosed in the stainless steel vacuum cryostat is 165 kg. The liquid xenon in the target volume is 65 kg, enclosed by a cylindrical PTFE and copper structure. PTFE reflects scintillation light (with high efficiency for VUV region [6]) and optically separates the target volume from the surrounding LXe, which has a mass of 100 kg ($\sim$4 cm thick). In addition to self-shield capability of LXe due to its high density, light sensors installed in the xenon volume around the target provide an active veto for additional background discrimination.

The TPC is installed in a double walled low activity stainless steel cryostat vessel sitting on the stainless steel support bars fixed to the shield door. The total weight of the vessel is 73.6 kg, which is only 30% of that of the XENON10 prototype [4].

Electrons created by ionization in the LXe target are drifted upwards by a strong electric field applied across the TPC. The cathode is located in the liquid phase below the target. In order to shield the bottom PMTs from the electric field, an additional (screening) mesh is installed below the cathode. The anode stack is placed in the gas phase maintained inside the 'diving bell' [7]. An extraction field is created across the liquid-gas interface by applying high voltage on the anode. Two additional meshes are installed below and above the anode and kept at ground potential, to close the field cage, and shield the top PMT array from the high electric field.

The scintillation light generated by particles interacting with the xenon atoms is detected by 242 one square inch R8520-06-Al Hamamatsu photomultiplier tubes (PMT). The top PMT array consists of 98 PMTs. 80 PMTs are immersed in liquid xenon below the target volume. Additionally, 64 PMTs view the veto volume: 16 PMTs above and below the TPC and 32 observing the sides.

## 3 Background Predictions

The background of the XENON100 experiment consists of two types: electron recoils (gamma, beta radiation) and nuclear recoils (elastic neutron scatters).

Electron recoil background originates from radioactive contamination of detector and shield materials ($^{232}$Th, $^{238}$U, $^{60}$Co, and $^{40}$K), radioactive contamination in liquid xenon ($^{232}$Th, $^{238}$U and $^{85}$Kr), and the decays of $^{222}$Rn and its progeny inside the shield cavity.

The main source of nuclear recoil background is neutron production with ($\alpha$,n) reactions from $^{232}$Th, $^{238}$U, and $^{235}$U decays and spontaneous fission of $^{238}$U in materials of the detector, shield and rock and concrete of the underground laboratory. Another contribution comes from muon-induced neutrons.

The majority of materials planned to be used in the construction of the XENON100 detector and its shield were screened with low background Ge detectors in order to determine their radioactivity. Table 1 shows the results of the measured radioactive contamination, including contamination in LXe, determined with a $\beta$-$\alpha$ delayed coincidence technique.

These values are used as an input information for the Monte Carlo simulations with GEANT4 toolkit and predictions of the background from various sources.

Dangerous background comes only from single scatter events, as this is the predicted behavior of a WIMP. Multiple scatter events are rejected taking into account the position resolution of the detector.

The fiducial volume cuts used in the analysis of the Monte Carlo data are preliminary, as appropriate for such a study. In addition, the effect of the active veto is not considered in the

Table 1: Radioactive contamination of the materials used in the construction of XENON100. The PMT signal cables additionally contain (5.0±0.9) mBq/kg of $^{108m}$Ag. Lead used for the shield is contaminated with $^{210}$Pb: (530±70) Bq/kg in the outer layer and (26±6) Bq/kg in the inner layer.

| **Material** | **Unit** | **$^{238}$U [mBq/unit]** | **$^{232}$Th [mBq/unit]** | **$^{60}$Co [mBq/unit]** | **$^{40}$K [mBq/unit]** |
|---|---|---|---|---|---|
| Stainless steel | kg | < 1.7 | < 1.9 | 5.5±0.6 | < 9.0 |
| PTFE | kg | < 0.31 | < 0.16 | < 0.11 | < 2.25 |
| PMTs | piece | 0.15±0.02 | 0.17±0.04 | 0.6±0.1 | 11±2 |
| PMT bases | piece | 0.16±0.02 | 0.07±0.02 | <0.01 | <0.16 |
| Support bars (steel) | kg | < 1.3 | 2.9±0.7 | 1.4±0.3 | < 7.1 |
| Copper (inside) | kg | < 0.22 | < 0.16 | 0.20±0.08 | < 1.34 |
| Resistor chain | piece | 0.027±0.004 | 0.014±0.003 | < 0.003 | 0.19±0.03 |
| Cathode support ring | kg | 3.6±0.8 | 1.8±0.5 | 7.3±1.3 | < 4.92 |
| Top grids support rings | kg | < 2.7 | < 1.5 | 13±1 | < 12 |
| PMT signal cables | kg | < 1.6 | 3.7±1.8 | < 0.69 | 35±13 |
| Polyethylene shield | kg | 0.23±0.05 | < 0.094 | < 0.89 | 0.7±0.4 |
| Copper shield | kg | < 0.07 | < 0.03 | < 0.0045 | < 0.06 |
| Lead shield (outer) | kg | < 0.92 | < 0.72 | < 0.12 | 14±3 |
| Lead shield (inner) | kg | < 0.66 | < 0.55 | < 0.11 | < 1.46 |
| Liquid xenon | | < 2.90 ppt | < 1.95 ppt | | |

present analysis. For the detailed study, see [8].

The total single nuclear recoil rate, from all sources listed in table 2, is 1.43 (0.55) event/year for 50 kg (30 kg) fiducial volume. It is dominated by the neutrons originating from the radioactive contamination in the detector, shield, and laboratory materials It is concluded that no muon veto is required for the XENON100, but will be relevant in the next generation of the XENON dark matter experiments.

Table 2: Nuclear recoil background.

| | **Single nuclear recoils per year in** | |
|---|---|---|
| | **50 kg FV** | **30 kg FV** |
| Detector and shield materials | $< 0.68$ | $< 0.28$ |
| Cavern | $0.48 \pm 0.15$ | $0.20 \pm 0.09$ |
| Cosmic ray muons | $0.27 \pm 0.13$ | $< 0.07$ |
| All sources | $< 1.43$ | $< 0.55$ |

The dominant background of the XENON100 dark matter search experiment is the electron recoil background. As it is shown in table 3, the main background source is radioactive contamination in the detector materials (dominated by PMTs). Background rate from beta-decay of $^{85}$Kr in liquid xenon is scaled to 0.7 ppb of Kr, the value determined with a delayed coincidence analysis before purification with a dedicated distillation column, which is expected to reduce krypton concentration down to ppt level [9].

Table 3: Electron recoil background.

| | **events/(kg·day·keVee)** | |
|---|---|---|
| | **50 kg FV** | **30 kg FV** |
| Detector and shield materials | $< 21.01$ | $< 7.73$ |
| $^{238}$U and $^{232}$Th in LXe | $<5.57$ | $<3.24$ |
| $^{85}$Kr in LXe | $< 11.85$ | $< 7.05$ |
| $^{222}$Rn in the cavity | $< 2.56$ | $< 1.24$ |
| All sources | $< 40.99$ | $< 19.26$ |

## References


[1] E. Aprile, L. Baudis, arXiv:0902.4253 (2008).

[2] G. Steigman and M.S. Turner, Nucl. Phys. **B253** 375 (1985).

[3] D. Clowe *et al.* Astrophys. J. **648** L109 (2006).

[4] J. Angle *et al.* (XENON10 Collaboration), Phys. Rev. Lett. **100**, 021303 (2008).

[5] T. Doke *et al.*, NIM **A420** 62 (1999).

[6] M. Yamashita *et al.*, NIM **A535** 692 (2004).

[7] J. Angle *et al.* (XENON10 Collaboration) 'Design and performance of the XENON10 dark matter experiment'. In preparation.

[8] E. Aprile *et al.* 'A Monte Carlo study of the electron and nuclear recoil background for the XENON100 dark matter search experiment'. In preparation.

[9] K. Abe *et al.* (XMASS Collaboration), Astrop. Phys. **31**, 290 (2009).